

See discussions, stats, and author profiles for this publication at: <https://www.researchgate.net/publication/270464839>

Automatic detection and classification of weld flaws in TOFD data using wavelet transform and support vector machines

Article in *Insight - Non-Destructive Testing and Condition Monitoring* · November 2010

DOI: 10.1784/insi.2010.52.11.597

CITATIONS

8

READS

161

4 authors:



Ali Al-Ataby

University of Liverpool

38 PUBLICATIONS 266 CITATIONS

[SEE PROFILE](#)



Waleed Al-Nuaimy

University of Liverpool

163 PUBLICATIONS 1,434 CITATIONS

[SEE PROFILE](#)



Colin R Brett

Uniper Technologies Ltd

24 PUBLICATIONS 112 CITATIONS

[SEE PROFILE](#)



O. Zahran

Menoufia University

112 PUBLICATIONS 551 CITATIONS

[SEE PROFILE](#)

Some of the authors of this publication are also working on these related projects:



ECG signal compression [View project](#)



Workflow management systems [View project](#)

Automatic detection and classification of weld flaws in TOFD data using wavelet transform and support vector machines

A Al-Ataby, W Al-Nuaimy, C R Brett and O Zahran

Submitted 27.04.10

Accepted 12.10.10

Ultrasonic time-of-flight diffraction (TOFD) is known as a reliable non-destructive testing technique for the inspection of welds in steel structures, providing accurate positioning and sizing of flaws. The automation of data processing in TOFD is required towards building a comprehensive computer-aided TOFD inspection and interpretation tool. A number of signal and image processing tools have been specifically developed for use with TOFD data. These tools have been adapted to function autonomously, without the need for continuous intervention through automatic configuration of the critical parameters according to the nature of the data and the acquisition settings. This paper presents several multi-resolution approaches employing the wavelet transform and texture analysis for de-noising and enhancing the quality of data to help in the automatic detection and classification of defects. The automatic classification is implemented using a support vector machines classifier, which is considered faster and more accurate than artificial neural networks. The results achieved so far have been promising in terms of accuracy, consistency and reliability.

1. Introduction

Non-destructive testing (NDT) is commonly used to monitor the quantitative safety-critical aspects of manufactured components and forms one part of quality assurance procedures. For applications such as the inspection of welded joints in steel structures, ultrasonic techniques are often the NDT method of choice. TOFD is one such technique, developed by Silk⁽¹⁾ in the late 1970s to improve the sizing accuracy of flaws. Currently, the critical stages of TOFD data processing and interpretation are still performed off-line by skilled operators. This is a time-consuming and painstaking process requiring high operator skill, alertness, consistency and experience.

The TOFD data acquisition and display configurations themselves may introduce a host of errors that cannot be accounted for by manual interpretation, leading to a reduction in the quality of the acquired data. Noise formed from scattering of inhomogeneous micro-structures and electronic circuitry is another source of

errors. Automatic data processing is often made difficult by this superimposed noise, as it can sometimes mask indications due to small but potentially dangerous defects^(2,3,4). The task of defect classification in noisy data is another critical challenge. Correctly identifying flaw categories has great importance in the process of decommissioning of work-pieces and structures through identifying the nature of flaws (serious or negligible).

In this paper, the wavelet transform is used as a method for de-noising to improve the quality of the acquired data. For classification, the support vector machines classifier is used to discriminate between defect classes with input features that also depend on the use of the wavelet transform. The data used to test the efficiency of the suggested methods is obtained from D-scan TOFD samples collected after applying TOFD on test plates, using ultrasonic probes of 5 MHz centre frequency with a sampling rate of 100 MHz and a collection step of 0.1 mm. The region of interest in this paper is the compression wave area that is enclosed between the lateral wave and the backwall echo.

2. Data quality enhancement and pre-processing

Raw TOFD data returns from the data acquisition process are in need of significant processing before being 'usable' for automatic defect evaluation, specifically when noise and other factors are present. The processing may include noise suppression (de-noising), scan alignment and accurate detection of the lateral wave^(2,3,4). These operations can be done in an automatic way to minimise the inconsistency and error introduced by human factors and without reducing the spatial resolution of the acquired data. Effective quality enhancement and pre-processing facilitate successful and accurate automatic defect detection and subsequent classification, positioning and sizing.

This section shows the role played by the wavelet transform and other important operations to improve the quality and consistency of the raw TOFD data to be used for automation and computer interpretation purposes.

2.1 De-noising and the MRA

The removal of noise from noisy data while preserving useful information is often referred to as de-noising. Due to its computational efficiency, multi-resolution analysis (MRA) is considered as a powerful tool in de-noising and to enhance the SNR of ultrasonic TOFD signals^(5,6,7).

The wavelet transform offers an inherent MRA that can be used to obtain the time-frequency representation of the ultrasonic signal. The de-noising procedure used in this paper is based on decomposing the signal using the discrete wavelet transform (DWT). The global dynamics of an NDT-related signal $f(t)$ are condensed in the wavelet approximation coefficients (WACs) that are related to the low frequencies. On the other hand, local oscillations of $f(t)$ (such as noise) are depicted in a set of so-called wavelet detail coefficients

A Al-Ataby and W Al-Nuaimy are with the Department of Electrical Engineering & Electronics, University of Liverpool, Liverpool L69 3GJ, UK. Tel: +44 (0)151 794 4580; Fax: +44 (0)151 794 4540; Email: aliataby@liv.ac.uk / wax@liv.ac.uk

C R Brett is with Inspection Management, E.ON Engineering Limited, Nottingham NG11 0EE, UK. Tel: +44 (0)24 7619 2313; Fax: +44 (0)115 902 4003; Email: colin.brett@eon-engineering.com

O Zahran is with the Department of Electronics & Communication Engineering, Menofia University, Menofia, PO Box 32952, Egypt. Tel: +20 48 3661334; Fax: +20 48 3660716; Email: osama_zahran@menofia.edu.eg

(WDCs) that are related to the high frequencies.

After the application of DWT to get the WACs and the WDCs, the next step is thresholding of some WDCs and reconstruction of the signal from the other WDCs and WACs using the inverse transform (IDWT). The method is a generalisation of wavelet decomposition that offers a larger range of possibilities for signal analysis. In normal wavelet analysis, a signal is split into WACs and WDCs. The approximation is then itself split into a second-level approximation and detail, and the process is repeated. In this analysis, the detail coefficients, as well as the approximation coefficients, can be split. This analysis is called the wavelet packet transform (WPT)^(6,7) (see Figure 1). Hard thresholding was employed with the threshold computed from WDCs at each level of decomposition based on the standard deviation as follows⁽⁷⁾:

$$\theta = k \sqrt{\frac{1}{N-1} \sum_{i=1}^N (D_i - \bar{D})^2} \dots\dots\dots(1)$$

where k is a factor related to the ratio of peak value to the RMS value, D_i is the WDC at each level and N is the length of each set of details coefficients.

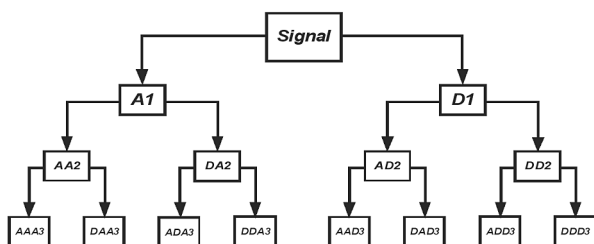


Figure 1. Discrete multi-resolution scheme – WPT: A is the approximation (low-pass) component and D is the detail (high-pass) component

In order to assess the quality of the suggested de-noising process, the SNR is computed for different defect samples. The obtained SNR values were calculated using the following equation⁽⁶⁾:

$$SNR_{dB} = 20 \cdot \log \left(\frac{S_{RMSF}}{N_{RMSN}} \right) \dots\dots\dots(2)$$

where S_{RMSF} is the RMS value of the filtered signal, and N_{RMSN} is the RMS value of the noise-only part of the raw signal.

In this paper, three decomposition levels are used with Daubechies (db6) as the wavelet filter. When compared with averaging or Wiener filtering, de-noising through wavelet transform returned higher SNR values. Figure 2 shows some D-scan samples before and after applying the wavelet de-noising method with the corresponding SNR. Although SNR improvement for human interpretation before and after applying de-noising may not appear significant, this improvement is more than adequate in terms of automation and computer interpretation. The performance of the subsequent processing stages shows remarkable enhancement after the de-noising process.

2.2 Other pre-processing steps

In addition to de-noising, the process of data quality enhancement includes other important operations to improve the quality and consistency of the data to enable accurate defect characterisation and positioning downstream. Scan alignment is one of these operations. A number of data acquisition factors may contribute to the misalignment of adjacent A-scans, including couplant thickness variations, surface irregularities, inadvertent changes in probe separation and accidental probe lift-off^(2,4). As the tips of the defects must be accurately located within the material and the lateral wave is used as reference points, aligning adjacent scans is essential. In this paper, scan alignment is carried out by cross-correlating each

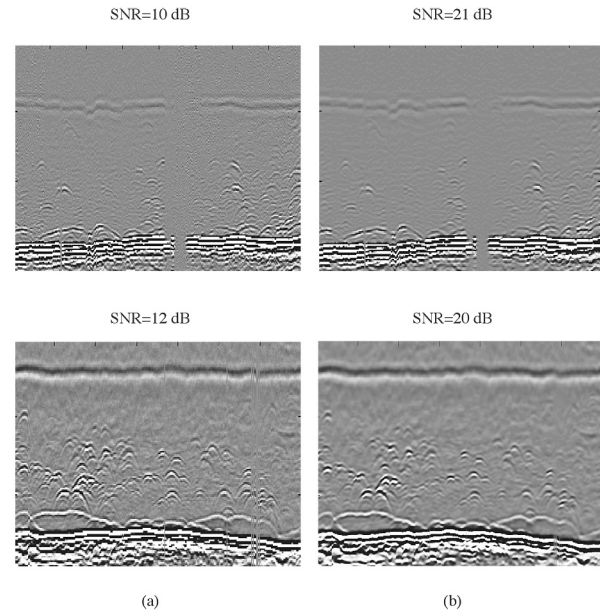


Figure 2. Wavelet de-noising. Scans of column (a) are before de-noising and (b) are after de-noising with their corresponding SNR values

scan with an arbitrary ‘reference’ scan (first A-scan in the image). The positions of the peaks in these cross-correlation plots are used to automatically shift each A-scan forward or backward in time in such a way as to align the envelope of the lateral wavelets. This not only influences the profile of the lateral wave, but also the shapes of the defect signatures themselves.

Automatic detection of the lateral wave is another essential pre-processing operation. The lateral wave is an important reference point, specifically when sizing and positioning is considered. It is also needed for scale linearisation and calibration. To detect the lateral wave, the first major wavelet peak (or trough, depending on the phase) of the aligned A-scans is detected.

3. Automatic flaw detection based on MRA-WPT and fuzzy logic

This section illustrates some techniques that are followed in this paper to detect flaws automatically. MRA based on WPT along with texture analysis are used to select (or filter) the image(s) to be used in the automatic detection process. Image segmentation is then used to highlight and enclose defects inside windows (called defect blobs). Segmentation can be done by statistical methods (for example variance thresholding) or through computational intelligence methods (in this case, fuzzy logic). The output of this step is a group of segmented defect blobs that are ready for further analysis and classification.

3.1 MRA-WPT for image filtering (selection)

As mentioned previously, the application of MRA to DWT is referred to as the wavelet packet transform (WPT), which is a signal analysis tool that has the frequency resolution power of the Fourier transform and the time resolution power of the wavelet transform^(3,5,7). It can be applied to time-varying signals, where the Fourier transform does not produce useful results and the wavelet transform does not produce sufficient results. The WPT can be considered an extension to the DWT, providing better reconstruction. In the wavelet packet framework, compression and de-noising ideas are exactly the same as those developed in the wavelet framework. The only difference is that WPT offers more complex and flexible analysis, as the details as well as the approximations are split⁽³⁾ (refer to Figure 1). The tree decomposition in the wavelet packet analysis can be applied continuously until the desired coarser resolution is reached.

A single wavelet packet decomposition gives different bases from which the best representation, with respect to a design objective, can be selected. This can be done by finding the best tree based on an entropy criterion⁽³⁾. Selection can also be done based on texture analysis and statistical contents of the obtained images. Wavelet packet analysis is used in this paper in two more important areas. The first area is to aid in detection (hence segmentation) of flaws based on fuzzy logic thresholding. The second area is to provide a ground for selecting defect blob features to be used as inputs to the SVM classifier in the classification stage (this will be explained later). Both areas rely on the powerful compression ability of the wavelet transform in general and WPT in particular to extract relevant and descriptive features.

The application of WPT to the D-scan images was carried out to analyse the scan image into multiple decomposition levels using the Debauchies of order 8 (db8), chosen as the most suitable analysing mother function in the wavelet packet filtering process. The chosen level of decomposition is three, since it achieved the required coarse resolution and higher decomposition levels would not add any significance to the analysis. First, the D-scan image is decomposed by the WPT (db8, L=3) in the first level. The grey-level co-occurrence matrix (GLCM) $P(i,j)$ is then calculated for the decomposed images. The descriptors or features that characterise the content of GLCM are calculated. The following are the three descriptors that are used in selection of the images for reconstruction⁽⁸⁾:

$$\square \text{ Contrast: } \sum_{i,j} |i-j|^2 p(i,j) \dots\dots\dots(3)$$

$$\square \text{ Energy: } \sum_{i,j} [p(i,j)]^2 \dots\dots\dots(4)$$

$$\square \text{ Entropy: } -\sum_{i,j} p(i,j) \cdot \log(p(i,j)) \dots\dots\dots(5)$$

where $p(i,j)$ is the normalised GLCM $P(i,j)$.

Based on these three descriptors, the image with the weakest textural information is discarded, and the one with the highest statistical contents is selected. After that, another decomposition level runs to generate the new set of images. The calculation of the descriptor commences again. The process of decomposition proceeds until level 3, and the final image is reconstructed from three images carrying the highest statistical textural information in the last level. This image is the key input to the next stages.

The above processing has shown to be effective in generating filtered scan images that are rich in its textural and statistical contents, showing only relevant details and indications. Hence, segmentation and classification of flaws have been affected positively in terms of performance, consistency and accuracy.

3.2 Segmentation through fuzzy logic

The segmentation technique used in this paper to extract defect blobs is based on the use of fuzzy logic, namely the fuzzy c-means iterative (FCMI) algorithm⁽⁹⁾. This method has shown better performance in terms of accuracy and automation than others, which are based on the statistical thresholding concept. The method is suitable to distinguish between superimposed defects when normal means (via trained operator or statistical methods) fail. The input to this algorithm is the final filtered image after MRA-WPT (explained in the previous section). The algorithm acts as a binarisation operation, with black pixels (values set to zeros) representing background and white pixels (values set to ones) representing flaws. This image (or mask in this case) is used to segment the input image after some further processing. Segmentation through the FCMI algorithm is a method that can be implemented as supervised or unsupervised. In this paper, unsupervised implementation is used. The details of the implementation of this method to segment the defect in TOFD images are out of the scope of this paper.

For better representation of the detected defects, each defect blob is represented in the form of a rectangle outlining the defect. This is achieved by applying a global thresholding of each defect blob separately in order to remove the lowest 10% of the pixel intensity values within the defect blob and then recording the minimum and the maximum spatial and temporal dimensions for each blob. This empirical threshold value proved to result in satisfactory performance for all the scan files considered. These recorded dimensions are used to generate a new mask, with each defect blob represented by a rectangular outline. The defect may consist of more than one segment. As every defect should be represented in one rectangular blob, this problem is overcome by merging the rectangular blobs related to the same defect based on the dimensions between different blobs⁽²⁾. After some processing, the output of this step is a segmented image data with highlighted defects areas or blobs. An example is shown in Figure 3.

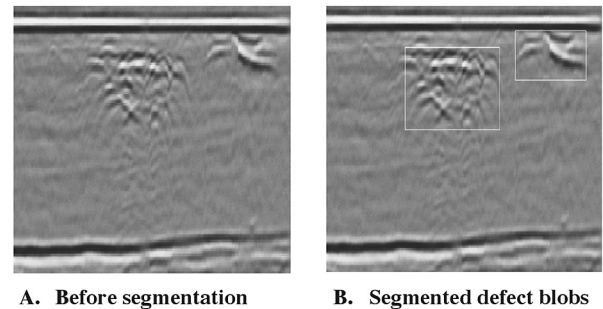


Figure 3. Automatic segmentation output

4. Automatic classification using SVM and wavelet features

In the context of supervised classification, machine learning and pattern recognition are the extraction of regularity or some sort of structure from a collection of data. Neural networks (NN) and Bayesian classifiers are typical examples to learn such organisation from the given data observations. The support vector machines (SVM) classifier is relatively new and is based on strong foundations from the broad area of statistical learning theory (SLT)⁽¹⁰⁾. The SVM classifier has become, in practice, the classifier of choice for numerous researchers because it offers several advantages which are typically not found in other classifiers, such as maximisation of generalisation ability, no local minima problem, low computational overhead, can work perfectly with lack of training data, robust with noisy data, does not suffer as much from the curse of dimensionality and prevents overfitting^(10,11).

4.1 The support vector machines

The SVM tries to maximise the margin between classes, and hence increases the generalisation ability. The SVM classifier is fundamentally developed for the binary classification case and is extendable for multi-class situations. The classification problem can be restricted to consideration of the two-class problem without loss of generality. The goal is to produce a classifier that works well on unseen examples.

The SVM classifier, like other linear classifiers, attempts to evaluate a linear decision boundary (assuming that the data is linearly separable) or a linear hyperplane between the two classes. Linearly separable data can be separated by an infinite number of linear hyperplanes. The problem is to find the optimal separating hyperplane (see Figure 4(a)) with maximal margin $M = 2/||W||$. It has been shown by Vapnik⁽¹⁰⁾ that this is a classical quadratic programming (QP) problem with constraints that ends in forming and solving of a Lagrangian. Once the Lagrange multipliers for the optimal hyperplane have been determined, a separating rule can be used in terms of support vectors and the Lagrange multipliers.

The concepts above are presented for a linear classification case. These are generalisable to a non-linear case, where a mapping function is used to map the input space into a higher dimensional feature space such that the non-linear hyperplane becomes linear by using a mapping function Φ , as shown in Figure 4(b). To avoid the increased computational complexity and the curse of dimensionality, a kernel trick or kernel function is employed which, in essence, computes an equivalent kernel value in the input space such that no explicit mapping is required. Kernels commonly used with kernel methods, and SVM in particular, are linear, polynomial and Gaussian radial basis function (RBF)^(10,11). In this paper, a multiclass SVM classifier is implemented using a one-against-all (OAA) method⁽¹⁰⁾, where the multi-class problem is reduced into multiple binary problems. A polynomial kernel of degree 5 is used in this implementation.

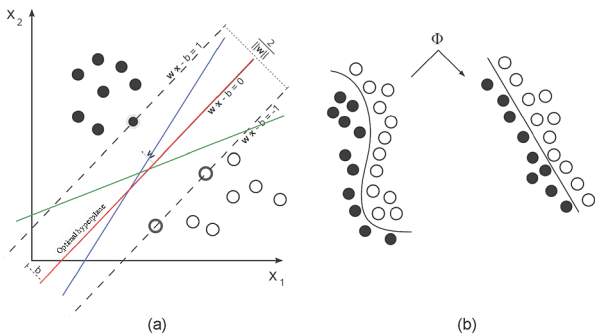


Figure 4. SVM classification concept: (a) Evaluation of an optimal hyperplane; (b) Feature mapping

4.2 Wavelet features

A large variety of feature extraction methods exist which are based upon signal processing (or filtering) techniques. Wavelet filtering is one such method that can be successfully used for feature extraction. The idea of using the wavelets for feature extraction in a classification context is not entirely new and has been applied before to texture analysis^(11,12); researchers have been using it for over a decade or so in one form or the other. The inherent capability to do so was highlighted on MRA using the wavelet transform. As explained before, wavelet transform decomposition and its extension, WPT, have gained popular applications in the field of signal/image processing. Wavelet transform enables the decomposition of the image into different frequency subbands, similar to the way the human visual system operates. This property makes it especially suitable for image segmentation and classification^(11,12). For the purpose of classification, appropriate features need to be extracted to obtain a representation that is as discriminative as possible in the transform domain. It is known that proper feature selection is likely to improve the classification accuracy with less number of features. A widely-used wavelet feature is the energy of each wavelet subband obtained after WPT⁽¹²⁾.

Two-dimensional WPT decomposition allows the analysing of an image simultaneously at different resolution levels. Different functions for energy can be used to extract features from each subband for classification. Commonly used energy functions include magnitude $|\bullet|$, magnitude

square $|\bullet|^2$ and the rectified sigmoid $\tanh(\bullet)$ ⁽¹²⁾. In this paper, the definition of energy based on squaring is used. The energy at different subbands is computed from the subband wavelet coefficient:

$$\sigma_p^2(k) = \sum_i \sum_j [C_k^p(i,j)]^2 \dots\dots\dots(6)$$

where $\sigma_p^2(k)$ is the energy of the obtained (decomposed) image projected onto the subspace at node (p,k) . The energy of each subband provides a measure of the image characteristics in that subband. The energy distribution has important discriminatory properties for images and as such can be used as a classification feature⁽¹²⁾.

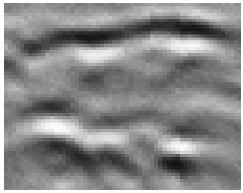
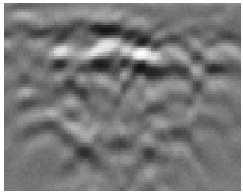
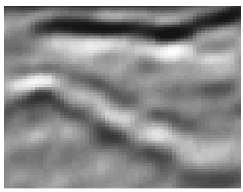
4.3 Discussions and results

This paper focuses on automatic detection and classification of three types of defect that are pure internal. These are clearly embedded and not open to or approaching either surface, and require advanced visual processing for interpretation. Apparent defects, on the other hand, such as upper crack, near surface slag and others, may be classified using geometrical and phase information alone^(2,13).

D-scan test samples containing 50 documented defects were used in the classification stage. The test samples and TOFD equipment are provided by Lavender International NDT Ltd. After applying the operations of Section 2 and 3 on the test samples, 50 defect blobs were obtained. The targeted defects for classification are summarised in Table 1, along with the corresponding number of samples for each defect type.

To train the SVM classifier, each defect blob sample is analysed by MRA-WPT with Daubechies 6-tap filter (db6) and a 3-level decomposition ($L=3$) to generate decomposition subbands. After each decomposition level, the energies are calculated. A feature vector of length 12, which contains energies (4 values per each level), is generated. It was found that by adding some regional features of each defect blob, the performance of the classifier was enhanced against the unseen defects. For that purpose, three regional features (after considering the defect blob as an image containing different-shaped regions and applying simple thresholding to it) are added to the wavelet feature vector, hence forming a final feature

Table 1. Defect samples used in the classification

Defect type	Symbol	Description	Code	Figure example	Available samples
Internal crack	IC	Shows up two echoes with some small irregularities between them.	1		15
Porosity	PO	A group of similar echoes with no resolvable length. Each echo shows only upper tip echo without the lower tip echo. Similar to patterns of acoustic noise and appears as a group of small arcs.	2		15
Large slag lines	SL	Shows as two echoes. The echo from the upper tip is larger in size and brighter than the echo from the bottom tip.	3		20

vector of 15 values. These three regional features are:

- ❑ Total number of islands: represents the number of the islands (segmented regions) in the absolute of the defect blob after thresholding.
- ❑ Number of positive islands: represents the number of the islands in the defect blob after thresholding.
- ❑ Relative area: represents the actual number of pixels in the regions of all islands divided by the area of the blob outlining all islands.

It should be noted that this feature vector of length 15 was found to be suitable for classification based on the defect types to be classified and the available samples (defined in Table 1). Larger feature vectors would be needed to classify more defect types to avoid overfitting.

The 50 defect blobs have been used to obtain different training and testing patterns. The output of the SVM classifier is a number which codifies each kind of defect as follows: 1 for IC, 2 for PO and 3 for SL. As mentioned previously, the SVM classifier has been trained using a 5-degree polynomial kernel implementing the OAA method for the case of study. At the end of the training phase, test patterns are applied and the SVM classifier returns a particular matrix, the so-called confusion matrix (CM)⁽³⁾, which evaluates the goodness of a trained classifier. Generally speaking, the element CM_{ij} of a CM is the probability that a single pattern belonging to the i -th class could be classified as belonging to the j -th class (the sum of elements of each row is therefore equal to 1). Thus, the more the CM is similar to the identity matrix, the better classification performance is. The other performance factors that were selected to assess the SVM classifier are the classification accuracy (CA) and the precision (P). In terms of CM elements, classification accuracy and precision are defined as follows:

$$CA = \frac{\sum_{i=1}^{nc} CM_{ii}}{nc} \times 100\% \dots\dots\dots(7)$$

$$P = \frac{1}{nc} \sum_{i=1}^{nc} \frac{CM_{ii}}{\sum_{j=1}^{nc} CM_{ji}} \times 100\% \dots\dots\dots(8)$$

where nc is the number of classes to be discriminated ($nc = 3$ in the present case).

Table 2 shows the resulting performance of the built SVM classifier for three different tests. It can be seen from this Table that after applying the built SVM classifier using 34%, 50% and 60% of the available defect samples for training, classification rates of

80%, 93% and 100% were obtained, respectively. Figure 5 is an output example of the classification stage.

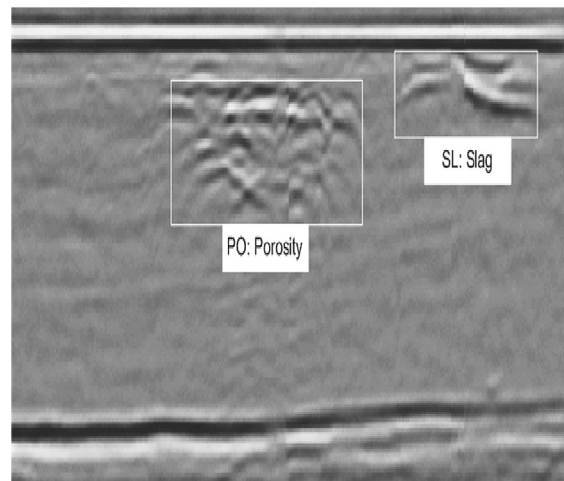


Figure 5. Automatic classification output

5. Conclusion

This paper has presented several promising methods to aid in the automation of detection and classification of flaws using TOFD, specifically when there is a lack of data quality. These methods are under development and need to be studied and tested thoroughly on real-life examples before being generalised and applied as reliable automatic interpretation methods. The following are the main conclusions and findings after applying the above methods:

- The de-noising of data (using wavelet transform) positively affects the detection accuracy and the performance of the classifier.
- The SVM classifier is robust and promising. It shows good performance when there is a lack of training data (which is not the case with other classifiers such as NN).
- The use of defect blobs wavelet features as inputs to the SVM classifier seems to be in favour of the overall classification performance.
- The response time of performing detection and classification processes using the proposed methods is relatively short compared to others (mainly, the time domain methods). This is because of the inherent data compression ability of wavelet transform that has been used in different stages of detection and classification.

The images under processing are smaller due to this compression, leading to fewer computations and hence less processing time.

Future work will be on utilising and extending the techniques mentioned in this paper to perform automatic defect sizing and positioning, with the possibility of making use of the mode-converted waves to add more advantage to the D-scan method. Also, the SVM classifier will be studied thoroughly and extended to classify other internal defect types, such as a small piece of slag (with single echo), lack of fusion, lack of penetration and others, with the possibility of generating different feature vectors utilising phase information of defect echoes and using principal component analysis (PCA) to reduce and select relevant features.

Table 2. Performance of the SVM classifier for different training and test patterns

	Defect	No of training samples	No of testing samples	Total	Classifier performance metrics
Test 1	IC	5	10	15	$CM = \begin{bmatrix} 0.6 & 0.0 & 0.4 \\ 0.0 & 0.9 & 0.1 \\ 0.1 & 0.0 & 0.9 \end{bmatrix}$ $CA = 80\%, P = 83\%$
	PO	5	10	15	
	SL	7	13	20	
Test 2	IC	8	7	15	$CM = \begin{bmatrix} 0.8 & 0.0 & 0.2 \\ 0.0 & 1.0 & 0.0 \\ 0.0 & 0.0 & 1.0 \end{bmatrix}$ $CA = 93\%, P = 94\%$
	PO	8	7	15	
	SL	9	10	20	
Test 3	IC	10	5	15	$CM = \begin{bmatrix} 1.0 & 0.0 & 0.0 \\ 0.0 & 1.0 & 0.0 \\ 0.0 & 0.0 & 1.0 \end{bmatrix}$ $CA = 100\%, P = 100\%$
	PO	10	5	15	
	SL	10	10	20	

Acknowledgement

The authors would like to express gratitude and appreciation to E.ON Engineering Technology Centre for their support and funding of this work, and also to Lavender International NDT Ltd for allowing the use of their D-scan samples in this paper.

References

1. M G Silk, 'The rapid analysis of TOFD data incorporating the provisions of standards', 7th European Conference on NDT, Nice, France, Vol 1, pp 25-29, May 1998.
2. O Zahran and W Al-Nuaimy, 'Automatic data processing and defect detection in time-of-flight diffraction images using statistical techniques', Insight, Vol 47, No 9, pp 538-542, September 2005.
3. M Cacciola, F C Morabito and M Versaci, 'Ultrasonic and advanced methods for non-destructive testing and material characterisation', World Scientific, Ch 21, pp 493-516, 2007.
4. J Charlesworth and J Temple, Engineering Applications of Ultrasonic Time-of-Flight Diffraction, RSP, 2nd edition, 2001.
5. A L Graps, 'An introduction to wavelets', IEEE Computational Sciences and Engineering, Vol 2, 1995.
6. V Matz, M Kreidl and R Smid, 'Signal-to-noise ratio improvement based on the discrete wavelet transform in ultrasonic defectoscopy', Acta Polytechnica, Vol 44, No 4, pp 61-66, 2004.
7. M C Robini, I E Magnin, H Cattin and A Baskurt, 'Two-dimensional ultrasonic flaw detection based on the wavelet packet transform', IEEE Transactions on Ultrasonics, Ferroelectrics and Frequency Control, Vol 44, 1997.
8. R Haralick, K Shunmugam and I Dinstein, 'Textural features for image classification', IEEE Transactions on Systems, Man Cybernetics, SMC, Vol 3, No 1, pp 610-621, 1973.
9. F Wong, R Nagarajan, S Yaacob, A Chekima and N E Belkhamza, 'An image segmentation method using fuzzy-based threshold', International Symposium on Signal Processing and its Applications (ISSPA), Vol 1, pp 144-147, August 2001.
10. V N Vapnik, The Nature of Statistical Learning Theory, Springer, 2nd edition, 2000.
11. K M Rajpoot and N M Rajpoot, 'Wavelets and support vector machines for texture classification', Proceedings of INMIC 2004, 8th International Multitopic Conference, pp 328-333, December 2004.
12. K Huang and S Aviyente, 'Wavelet feature selection for image classification', IEEE Transactions on Image Processing, Vol 17, No 9, pp 1709-1720, September 2008.
13. British Standards Institution, 'Guide to calibration and setting-up of the ultrasonic time-of-flight diffraction (TOFD) technique for the detection, location and sizing of flaws', BS 7706, December 1993.



SPECIALISED PRODUCTS QUALITY SOLUTIONS

Manufacturers of:

- Lead Intensifying Screens*
- Plastic Cassettes*
- Image Quality Indicators*
- Cassettes with Film*
- Radiation Warning Signs*

**RADIOGRAPHIC
ACCESSORIES LIMITED**

DURHAM LANE INDUSTRIAL PARK
STOCKTON-ON-TEES
CLEVELAND TS16 0RF
Telephone: 01642 790580
Fax: 01642 790420
Website: <http://www.radac.demon.co.uk>
Email: jack@radac.demon.co.uk

Enquiry No 011-06

Copyright of Insight: Non-Destructive Testing & Condition Monitoring is the property of British Institute of Non-Destructive Testing and its content may not be copied or emailed to multiple sites or posted to a listserv without the copyright holder's express written permission. However, users may print, download, or email articles for individual use.